HHS Public Access

Author manuscript

J Neurosci Res. Author manuscript; available in PMC 2017 July 17.

Published in final edited form as:

J Neurosci Res. 2009 November 15; 87(15): 3369–3377. doi:10.1002/jnr.22099.

Insulin-Like Growth Factor-I-Stimulated Akt Phosphorylation and Oligodendrocyte Progenitor Cell Survival Require Cholesterol-Enriched Membranes

Robert J. Romanelli, **Kedar R. Mahajan**, **Clifton G. Fulmer**, and **Teresa L. Wood***

Department of Neurology and Neurosciences, University Hospital Cancer Center, University of Medicine and Dentistry of New Jersey, New Jersey Medical School, Newark, New Jersey

Abstract

Previously we showed that insulin-like growth factor-I (IGF-I) promotes sustained phosphorylation of Akt in oligodendrocyte progenitor cells (OPCs) and that Akt phosphorylation is required for survival of these cells. The direct mechanisms, however, by which IGF-I promotes Akt phosphorylation are currently undefined. Recently, cholesterol-enriched membranes (CEMs) have been implicated in regulation of growth factor-mediated activation of the PI3K/Akt pathway and survival of mature oligodendrocytes; however, less is know about their role in OPC survival. In the present study, we investigate the role of CEMs in IGF-I-mediated Akt phosphorylation and OPC survival. We report that acute disruption of membrane cholesterol with methyl-β-cyclodextrin results in altered OPC morphology and inhibition of IGF-I-mediated Akt phosphorylation. We also report that long-term inhibition of cholesterol biosynthesis with 25-hydroxycholesterol blocks IGF-I stimulated Akt phosphorylation and cell survival. Moreover, we show that the PI3K regulatory subunit, p85, Akt, and the IGF-IR are sequestered within cholesterol-enriched fractions in steady-state stimulation of the IGF-IR and that phosphorylated Akt and IGF-IR are present in cholesterol-enriched fractions with IGF-I stimulation. Together, the results of these studies support a role for CEMs or “lipid rafts” in IGF-I-mediated Akt phosphorylation and provide a better understanding of the mechanisms by which IGF-I promotes OPC survival.

Keywords

insulin-like growth factor; signal transduction mechanisms; apoptosis; PI3K; Akt

Insulin-like growth factor-I (IGF-I) is essential for the survival and development of oligodendrocytes, the myelin-forming cells of the central nervous system (CNS). The deletion of the IGF-I gene in mice induces a marked decrease in total brain size as well as hypomyelination, with a reduced number of oligodendrocytes and oligodendrocyte progenitor cells (OPCs; Ye et al., 2002). Conversely, overexpression of IGF-I promotes brain overgrowth characterized by an increase in the number of oligodendrocytes as well as a

*Correspondence to: Teresa L. Wood, Department Neurology and Neuroscience, UH-Cancer Center H1200, New Jersey Medical School/UMDNJ, 205 S. Orange Ave., Newark, NJ 07101. woodte@umdnj.edu.

The first two authors contributed equally to this work.

marked increase in myelination (Carson et al., 1993; Ye et al., 1995). These mice also display an increase in the antiapoptotic protein Bcl-2 in the cerebral cortex and cerebellum and are consequently protected from demyelination induced by undernutritional insults compared with wild-type animals (Ye et al., 2000; Chrysis et al., 2001). Administration of exogenous IGF-I after experimental autoimmune encephalomyelitis (EAE), a model of multiple sclerosis (MS), promotes remyelination in rats (Yao et al., 1995). Interestingly, endogenous IGF-I is expressed during recovery from EAE as well as during recovery from cerebral ischemia and other forms of neurological trauma that particularly target oligodendrocytes and the white matter (Komoly et al., 1992; Gehrmann et al., 1994; Lee et al., 1996). Together, these data strongly suggest that IGF-I promotes the survival of oligodendroglia, contributes to proper myelination, and is protective during experimental models of injury in vivo.

IGF-I signals primarily through the IGF type-I receptor (IGF-IR) and is a potent activator of the phosphatidylinositol-3-kinase (PI3K)/Akt pathway, an essential survival pathway in numerous cell types (Stam et al., 2001; Lee et al., 2005). Consistently with the studies on IGF-I, loss of the IGF-IR in oligodendroglial-lineage cells results in decreased oligodendrocyte number and myelination in white matter. In addition, deletion of the IGF-IR in OPCs results in decreased proliferation (Zeger et al., 2007). Similarly to IGF-I, the IGF-IR is also essential for remyelination in mice (Mason et al., 2003). Our previous studies showed that IGF-I promotes survival and protection of OPCs in vitro from serum deprivation and glutamate toxicity through sustained phosphorylation of the IGF-IR and Akt (Ness et al., 2002). More recently, we demonstrated that internalization and recycling of IGF-IR are required for sustained IGF-I-stimulated Akt phosphorylation in OPCs (Romanelli et al., 2007). This study is consistent with other reports that receptor trafficking and subcellular targeting are necessary for the regulation of signal transduction pathways and resultant biological responses (Romanelli and Wood, 2008).

“Lipid raft” microdomains, thought to organize membrane proteins and mediate signal transduction, are enriched in cholesterol and sphingolipids (Simons and Ikonen, 1997). Their isolation by insolubility in cold nonionic detergent and buoyancy in sucrose density centrifugation presents an important biological means of accessing potential protein–”raft” association, although it does not dictate this association (Lingwood and Simons, 2007). These cholesterol-enriched membranes (CEMs) have been implicated in the regulation of the PI3K/Akt signaling pathway and trophic factor-mediated survival within oligodendrocytes. For example, platelet-derived growth factor (PDGF)-mediated Akt phosphorylation and survival of newly differentiated oligodendrocytes are enhanced through the colocalization of PDGF receptors and α6β1 integrins within CEMs (Decker and ffrench-Constant, 2004). These data are consistent with the notion that CEMs organize and compartmentalize receptors and signaling proteins (Gielen et al., 2006), promoting the specificity and fidelity of signaling events within the cell.

In the present study, we test the hypothesis that CEMs promote IGF-I-stimulated phosphorylation of Akt and survival of OPCs. We report that acute cholesterol depletion alters OPC membrane morphology and blocks IGF-I-mediated Akt phosphorylation. We also show that IGF-I-mediated Akt phosphorylation is cholesterol dose dependent and that

long-term inhibition of cholesterol biosynthesis results in a decrease in IGF-I-mediated survival. Finally, we demonstrate that the IGF-IR, IRS-1, PI3K regulatory subunit, p85, and Akt are sequestered within cholesterol-enriched fractions in OPCs and that IGF stimulation of OPCs results in increased P-IGF-IR and P-Akt in detergent-insoluble fractions. The results of these studies support a role for CEMs in IGF-IR signaling and provide a better understanding of the mechanisms by which IGF-I promotes the survival of OPCs.

MATERIALS AND METHODS

Materials

Cell culture medium (MEM, DMEMF-12) and fetal bovine serum (FBS) were purchased from Gibco-BRL (Grand Island, NY). Cholesterol, 25-hydroxycholesterol, protease inhibitors, methyl-β-cyclodextrin, 25-hydroxycholesterol, and additional cell culture materials were purchased from Sigma (St. Louis, MO). Recombinant human IGF-I was purchased from Upstate Biochemicals (Lake Placid, NY). Antibodies to total Akt, phosphorylated (Ser473)-Akt, and the phosphorylated IGF-I receptor β (Tyr1131)/insulin receptor β (Tyr1146) antibodies were purchased from Cell Signaling Technology (Beverly, MA). Antibodies to IGF-IRβ were purchased from Cell Signaling Technology or Santa Cruz Biotechnology (Santa Cruz, CA). The β-actin antibody and goat anti-rabbit and goat anti-mouse horseradish peroxidase (HRP)-conjugated secondary antibodies were purchased from Jackson Immunoresearch (West Grove, PA). The caveolin-1 antibody was purchased from Santa Cruz Biotechnology. The antibody to flotillin-1 was purchased from Transduction Laboratories (San Diego, CA). The PI3K regulatory subunit p85 antibody was purchased from Millipore (Billerica, MA). GM-1 ganglioside standard and cholera-toxin β-HRP conjugate were a kind gift from Dr. Robert Ledeen (UMDNJ, Newark, NJ).

Preparation of Primary Oligodendrocyte Progenitor Cultures

All animal experimentation protocols were approved by Penn State College of Medicine and the University of Medicine and Dentistry of New Jersey (UMDNJ) Institutional Animal Care and Use Committees (IACUC) and were conducted in accordance with the National Institutes of Health guidelines for the care and use of laboratory animals. OPCs were harvested from P0–P2 Sprague Dawley rats (Charles River Laboratories) as previously described (Levison and McCarthy, 1991). Briefly, forebrain cortices were enzymatically and mechanically dissociated, resulting in a mixed glial population of cells. Mixed glial cultures were grown for 12 days; OPCs were separated from astrocytes and microglia by differentially shaking and plating. Purified OPCs were maintained in N2S media composed of 1) 66% N2B2 media [DMEM/F-12 supplemented with 0.6 mg/ml BSA, 10 ng/ml d-biotin, 20 nM progesterone, 100 μM putrescine, 5 ng/ml selenium, 50 μg/ml apotransferrin, 100 U/ml penicillin, and 100 μg/ml streptomycin; 2) 34% B104 conditioning medium; 3) 5 ng/ml FGF-2; and 4) 0.5% fetal bovine serum. This preparation of OPCs consistently yields cultures that are >95% biopolar early OPCs ($A2B5^+/O4^-/GalC^-$). Cells were plated on poly-D-lysine-coated dishes at a density of 2.0×10^4 cells/cm^2 in N2S media for treatments. Prior to all treatments, cells were serum starved in N1A media (N2B2 without insulin or serum) for 2 hr.

Western Blot Analysis

After treatments, OPCs were washed in ice-cold PBS, and total cell lysates were isolated in SDS sample buffer (62.5 mM Tris-HCl, 2% SDS, 10% glycerol, 50 mM DTT) containing 1:100 protease inhibitor cocktail, 1 mM sodium orthovanadate, and 1 mM sodium fluoride (Sigma). Lysates were briefly sonicated on ice and quantified by the RC/DC protein assay (Bio-Rad, Hercules, CA). Approximately 20 μg of protein from each sample was boiled for 5 min, cooled, separated by SDS-polyacrylamide gel electrophoresis (PAGE) on 4–12% mini-gels (Invitrogen, Carlsbad, CA), and subsequently transferred to nitrocellulose membranes. Membranes were blocked in 5% milk in TBS-0.05% or 0.1% Tween for 1 hr and incubated with primary antibodies overnight at 4°C, with gentle rocking. Subsequently, membranes were incubated with appropriate goat anti-rabbit or goat anti-mouse HRP-conjugated secondary antibody for 1 hr at room temperature. The detection of HRP-conjugated secondary antibodies was performed with an enhanced chemiluminescence kit (ECL; New England Nuclear, Boston, MA) and an UltraLum imaging camera and software.

Cholesterol Depletion and Replacement

For acute depletion of cholesterol, OPCs were treated with 5 mM MβCD for 30 min at 37°C prior to trophic factor stimulation. Cells were rinsed twice with basal media and were subsequently treated with 10 ng/ml IGF-I for 30 min. Cholesterol was replaced as described previously (Klein et al., 1995). Briefly, 6 mg of cholesterol (Sigma) in 0.2 ml of isopropyl alcohol was added to 100 mg/ml MβCD at 80°C, yielding a 6.8 mM cholesterol-MβCD solution. Cholesterol complexes were diluted into treatment media to a final concentration of 0.2 mM and were incubated for 30 min at 37°C. For inhibition of de novo cholesterol synthesis, OPCs were treated with either 1 μg/ml 25-hydroxycholesterol or ethanol vehicle control in basal media in the presence of IGF-I (10 ng/ml) for 24 or 30 hr.

Lubrol WX-Resistant Membrane Isolation

For CEM isolation by density centrifugation, OPCs from five 15-cm dishes at ~70% confluence in N2S were washed in cold PBS (without divalent cations) and scraped into MES homogenization buffer (MBS; 25 mM MES, 150 mM NaCl, pH 6.5) with protease inhibitors. The cells were then incubated with 0.5% of the nonionic detergent Lubrol WX 17A17 (Serva, Heidelberg, Germany), homogenized by passage through a 23-g 3-in. needle 20 times, and incubated for 30 min on ice. Equal volumes (1 ml) of lysate and 80% (w/v) sucrose/MBS were mixed and loaded into the bottom of polyallomer ultracentrifuge tubes. Samples were overlaid with 2 ml 35% sucrose/MBS and 1 ml 5% sucrose/MBS. Gradients were centrifuged at 46,900 rpm on a Sorvall AH-650 rotor at 4°C for 18 hr. Nine equal volume fractions (550 μl) were collected and loaded onto a 10-well 10% Bis-Tris gel for PAGE and Western blot analysis.

For crude CEM isolation, OPCs from 20 10-cm dishes at ~70% confluence in N2S were serum starved in N1A media for 2 hr prior to 15 min of exposure to either 20 ng/ml IGF-I in N1A or N1A alone. Dishes were washed in cold PBS and scraped into 1 ml TNE buffer (25 mM Tris-HCl pH 7.5, 150 mM NaCl, 5 mM EDTA) containing 0.238 mg/ml DNase, 0.385% (w/v) $MgSO_4$, and protease inhibitors. Cells were passed though a 27-g 3-in. needle 20 times and centrifuged at 1,000*g* for 5 min at 4°C to pellet nuclei/debris. The postnuclear

supernatant was incubated with 0.5% Lubrol WX on ice for 30 min, with vortexing every 5 min. The lysate was centrifuged at 13,000*g* for 20 min at 4°C min to pellet the Lubrol-insoluble fraction from the soluble supernatant. The soluble supernatants were mixed with 2 volumes of ethanol and placed in −20°C overnight to precipitate protein. The protein was pelleted the next day by centrifuging 25,000*g* for 20 min at 4°C. The Lubrol-insoluble and -soluble fractions were resuspended in a solubilization buffer containing 50 mM Tris-HCl, pH 6.8, 2.5% glycerol, 5% SDS, and 4 M urea and sonicated. After a protein assay, equal protein fractions were loaded on a 10-well 4–12% Bis-Tris gel for PAGE and Western blot analysis.

Total cholesterol was measured by the fluorometric Amplex Red Cholesterol Assay Kit (Molecular Probes, Eugene, OR) using a Victor^{3}V Multilabel Plate Counter (Perkin Elmer, Boston, MA). Total protein content was measured by the DC protein assay (Bio-Rad).

Statistical Analyses

Analyses were performed in Statview statistical software. One-way ANOVA followed by a Fisher's post hoc test was used for multiple-group comparisons. Data were analyzed by Student's *t*-test for two-group comparisons. $P < 0.05$ was considered statistically significant.

RESULTS

MβCD Alters the Integrity of OPC Membranes and Raft Microdomains

The cholesterol chelating agent MβCD classically is used to disrupt CEMs in living cells. To determine its effects on OPC morphology, we treated cells with 5 mM MβCD for 30 min at 37°C and examined cellular morphology by phase-contrast microscopy. Whereas untreated progenitors had normal and continuous bipolar processes extending from their cell body (Fig. 1A), treatment with MβCD resulted in progenitors with punctate and discontinuous processes (Fig. 1B). To ensure that the effects of MβCD were specific to cholesterol depletion, we replaced cholesterol after drug treatment. Alone, MβCD strips membranes of cholesterol; however, when complexed with cholesterol, MβCD is a vehicle for cholesterol replacement (Klein et al., 1995). With this experimental paradigm, progenitors were incubated with 200 μM cholesterol–MβCD complexes after MβCD treatments. After incubation with cholesterol, OPC membranes were indistinguishable from untreated cells (Fig. 1C). These results suggest that MβCD induces morphological changes in OPC membranes that are specific to cholesterol depletion.

Acute Cholesterol Depletion Blocks IGF-I-Mediated Akt Phosphorylation

Previous studies imply a role for CEMs in the regulation of the PI3K/Akt pathway and trophic factor signaling in multiple cell types, including mature oligodendrocytes (Decker and ffrench-Constant, 2004). Accordingly, we were interested in determining the role of membrane microdomains in IGF-I-mediated Akt phosphorylation in OPCs. Primary OPC cultures were stimulated with IGF-I for 30 min in serum-free media, with or without pretreatment with MβCD. Stimulation with IGF-I induced a significant increase in Akt phosphorylation compared with untreated cells ($P < 0.0001$; Fig. 2A,B). Pretreatment with MβCD, however, blocked IGF-I-mediated Akt phosphorylation. To determine that the

effects of MβCD were specific to the loss of cholesterol, cholesterol was replaced after MβCD treatment as previously described. Replacement of cholesterol rescued IGF-I-mediated Akt phosphorylation ($P < 0.0001$; Fig. 2A,B). In contrast, the phosphorylation of the IGF-IR after IGF-I stimulation, in both the presence and the absence of MβCD pretreatment, was similarly increased compared with untreated cells ($P < 0.03$; Fig. 2C,D). To determine further whether cholesterol is involved in IGF-I-mediated Akt phosphorylation, we treated OPCs with 0, 100, or 200 μM cholesterol complexes after pretreatment with MβCD. IGF-I-mediated Akt phosphorylation correlated with the dose of cholesterol (Fig. 2E,F). Together, the results of these studies suggest that cholesterol is required for IGF-I-mediated Akt phosphorylation but not the phosphorylation of the IGF-IR.

Inhibition of De Novo Cholesterol Biosynthesis Blocks IGF-I-Mediated Sustained Akt Phosphorylation and OPC Survival

The previous results demonstrate that acute depletion of cholesterol blocks short-term IGF-I-mediated Akt phosphorylation. Thus, we were interested in determining the long-term effects of cholesterol depletion on the phosphorylation of Akt. Because MβCD is toxic to cells in long-term assays, various inhibitors of cholesterol synthesis are commonly used for long-term cholesterol depletion studies. Accordingly, we used 25-hydroxycho-lesterol (25-HC), a well characterized and potent inhibitor of cholesterol biosynthesis for cells in culture. 25-HC suppresses cleavage of N-terminal fragments contained in sterol regulatory element-binding protein and therefore inhibiting transcription of cholesterol synthesis genes such as HMG-CoA synthase (Nishimura et al., 2005). Importantly, 25-HC was used previously to block cholesterol biosynthesis in Schwann cells (Fu et al., 1998). OPCs were treated with or without 25-HC for 24 or 30 hr in serum-free media in the continual presence of IGF-I. In these experiments, we observed a significant decrease in IGF-I-mediated Akt phosphorylation in groups treated with 25-HC for 24 hr ($P < 0.001$, Fig. 3A,B). By 30 hr, phosphorylation of Akt was still reduced in the 25-HC-treated cells vs. control cells, but the responsiveness to IGF-I appears diminished, likely because of increased differentiation of the cells in the absence of mitogens (Ness et al., 2002). Consistently with reduction in Akt phopshorylation, we observed a concomitant increase in caspase-3 cleavage at 24 hr ($P = 0.03$) and 30 hr ($P = 0.04$; Fig. 3A,C). Importantly, 25-HC had no significant effects on basal levels of Akt phosphorylation (Fig. 3A,B). Together, these data demonstrate that the inhibition of cholesterol biosynthesis blocks IGF-I-stimulated Akt phosphorylation and OPC survival.

Membrane Localization of the IGF-IR and Signaling Components

To investigate further the role of CEMs in IGF-I-mediated Akt activation, we subjected OPCs to membrane extraction with the nonionic detergent Lubrol WX, followed by sucrose density centrifugation. This method exploits the resistance of cholesterol-enriched liquid-ordered domains to detergent extraction and their buoyancy by distribution at the 5/35% sucrose interface (fractions 2 and 3). In initial studies, we compared different lipid raft extraction methods for OPCs, because there are known variations in selectivity of membrane protein/lipid extraction between cell types and detergents (Schuck et al., 2003). We found enrichment of cholesterol content in buoyant (raft) fractions using 0.5% Lubrol WX (Vetrivel et al., 2004) but not 1% Triton X-100 (Fig. 4B, and data not shown). Moreover,

flotillin-1 was distributed predominantly in fractions 2 and 3 with 0.5% Lubrol WX but was mostly in nonraft fractions with a 1% Triton X-100 method (Baron et al., 2003) or a sodium carbonate detergent-free method (Song et al., 1996; Macdonald and Pike, 2005; data not shown). We determined, based on these analyses, that the Lubrol WX method can be used for analyzing cholesterol-enriched fractions in OPCs.

By using the Lubrol WX method to analyze IGF-IR and signaling components in cholesterol enriched fractions, we observed a portion of the IGF-IR, the PI3K regulatory subunit p85, and Akt in the buoyant fractions during steady-state activation of the IGF-IR (Fig. 4A). The segregation of the plasma transmembrane protein flotillin-1 and GM-1 ganglioside and the absence of the endoplasmic reticulum membrane protein cal-nexin were used to identify raft fractions (Fig. 4A; Schuck et al., 2003; Hur et al., 2008). Total cholesterol (μg/ml) was enriched in the buoyant fractions (Fig. 4B). In contrast, the bulk of protein was distributed in the high-density fractions (Fig. 4B). Because the analysis was performed with equal volumes from each fraction, the reduced levels of protein in the buoyant fractions suggests that the IGF-IR is enriched in raft vs. nonraft membrane domains.

To obtain sufficient protein to detect IGF-I-mediated phosphorylation of Akt and the IGF-IR in CEMs, we isolated crude Lubrol-insoluble fractions enriched in cholesterol and caveolin-1 (Fig. 4C,D) by using a modified protocol established by Steven Pfeiffer (Marta et al., 2004, 2008). Increased levels of P-IGF-IR and P-Akt were observed in the insoluble fractions after stimulation of the OPCs by IGF-I for 15 min (Fig. 4C). In contrast, the total levels of IGF-IR, p85, and Akt appear to be unchanged in the insoluble fractions after IGF stimulation. Interestingly, the amount of total IGF-IR was higher in the insoluble than in the soluble fractions, which is generally consistent with the conclusion from the data shown in Figure 4A that the IGF-IR is enriched in raft fractions.

DISCUSSION

Our previous studies demonstrated that IGF-I stimulation of OPCs through the IGF-IR activates PI3K/Akt (Ness and Wood, 2002; Ness et al., 2004). The downstream consequences of IGF-IR/PI3K/Akt activation in OPCs include positive regulation of cell cycle components such as cyclin D1 (Frederick and Wood, 2004; Frederick et al., 2007) and negative regulation of proapoptotic Bcl family members such as Bax (Ness et al., 2004). Moreover, we demonstrated that stimulation of the IGF-IR results in sustained phosphorylation of Akt via trafficking of the IGF-IR through a recycling pathway and that this sustained Akt phosphorylation is important for long-term survival of OPCs from trophic factor deprivation or glutamate excitotoxicity (Ness and Wood, 2002; Romanelli et al., 2007).

In the current study, we show that cholesterol chelation by MβCD alters OPC morphology and blocks IGF-I-mediated Akt activation, but not IGF-IR auto-phosphorylation. Similarly, long-term inhibition of de novo cholesterol synthesis by 25-HC also decreases IGF-I-mediated Akt activation, with a concomitant increase in cleaved caspase 3. Conversely, the treatment of OPCs with increasing concentrations of cholesterol increases IGF-I-mediated Akt activation in a dose-dependent manner. Finally, we show that the IGF-IR and the PI3K

subunit p85 and Akt are detected in cholesterol-rich membrane domains under conditions of steady-state IGF-IR activation and that phosphorylated Akt and IGF-IR are detected in CEMs with IGF-I stimulation.

It is well characterized that subcellular compartmentalization of receptor tyrosine kinases and their downstream effectors regulates the differential activity of signal transduction pathways and leads to diverse biological responses (Romanelli and Wood, 2008). Most studies report that the PI3K/Akt and PKC pathways are activated exclusively at the plasma membrane because of the restricted availability of phosphatidylinositol (4,5)-bis-phosphate (PIP2), whereas the ERK pathway is activated at both the plasma membrane and the endosome as a result of global accessibility of its upstream signaling partners (Haugh and Meyer, 2002). Much attention has been paid to the localization of RTKs and their signaling partners at the plasma membrane vs. the endosome; however, less attention has been given to the spatial organization of these signaling proteins at the plasma membrane.

The emerging and established literature has implicated lipid raft microdomains in the organization of proteins for signal transduction and cellular function. Several studies support the notion that growth factor-mediated survival, likely through Akt, requires CEMs in neural cell types. The PDGFα receptor was shown to interact with α6β1 integrin in lipid rafts to promote survival via PI3K/Akt activation in newly differentiated oligodendrocytes (Baron et al., 2003). In that study, Baron and colleagues also showed that disruption of CEMs with the sphinogolipid synthesis inhibitor fumonisin B blocked PDGFα receptor and α6β1 integrin colocalization and resulted in decreased PDGF-mediated survival. In PC12 and rat cerebellar granule cells, the IGF-IR was shown to require caveolae, a subset of CEMs, for IGF-I-mediated survival (Lu et al., 2008).

CEMs also function in oligodendrocyte morphology at the onset of myelination through interactions with actin-binding proteins (Taguchi et al., 2005). Moreover, CEMs are important for the delivery of myelin-specific proteins to myelin membranes (Lee, 2001; Marta et al., 2003) and provide the structural organization within these specialized membranes (Kramer et al., 2001). Notably, mice deficient in oligodendrocyte-specific cholesterol biosynthesis display dysmyelination, tremors, and ataxia (Saher et al., 2005). Together, these data support the importance of cholesterol in normal myelination and myelin function. Consistently with these studies, here we show a role for cholesterol in morphology of the earlier oligodendrocyte-lineage stages.

In the present study, we have further developed our model of the mechanism by which IGF-IR regulates Akt phosphorylation and promotes survival of OPCs. In this model, we propose that compartmentalization of the IGF-IR in cholesterol-enriched microdomains is important for IGF-I-mediated Akt phosphorylation. Interestingly, cholesterol is not required for autophosphorylation of the receptor, because depletion of cholesterol did not disrupt IGF-mediated IGF-IR phosphorylation. However, we did observe an increase in P-IGF-IR in detergent-insoluble membrane fractions following IGF-I stimulation. Furthermore, we detected the IGF-IR, p85, and Akt in CEMs in OPCs during steady-state stimulation of the IGF-IR (standard media with micromolar levels of insulin that activate the IGF-IR) and phosphorylated IGF-IR and Akt with IGF-I stimulation. Moreover, we show that activation

of Akt by IGF-I occurs in CEMs, providing support for the hypothesis that these molecules associate functionally in these domains.

It is tempting to speculate that IGF-IR activates both cholesterol-dependent and cholesterol-independent signaling pathways and that sequestration of the receptor into distinct membrane domains (e.g., lipid rafts, non-rafts, recycling endosomes) aides in the regulation of IGF-IR-induced signaling events and biological outcomes. For example, in preadipocytes, acute cholesterol depletion results in an increase in IGF-I-mediated ERK phosphorylation but a decrease in Akt phosphorylation, which, respectively, correlate with enhanced IGF-I induced mitogenesis and decreased protection from toxic insults (Matthews et al., 2005). Although we did not determine whether cholesterol depletion enhanced IGF-I mediated ERK phosphorylation in OPCs in the current study, previously we found that IGF-I has no effect on ERK phosphorylation in purified rat OPCs (Frederick et al., 2007). Rather, IGF-I acts through the PI3K/Akt pathway to promote OPC survival as well as to enhance proliferation in coordination with fibroblast growth factor-2 (Frederick et al., 2007). The idea that these diverse functions of IGF-I might involve receptor signaling through distinct membrane domains is supported by results of a recent study indicating that Akt activated in nonraft domains is dependent on raft-activated Akt following IGF-I, but not PDGF, stimulation of NIH 3T3 cells (Gao and Zhang, 2008). These findings raise the interesting possibility that IGF-IR signaling in one domain may influence signaling in another domain either by the IGF-IR or by other receptors. It will be of interest for future studies to determine whether activation of the IGF-IR in different membrane domains leads to different biological actions of IGF-I and to determine the mechanisms for IGF-IR localization and signaling to CEMs in OPCs.

Acknowledgments

Contract grant sponsor: National Institute of Neurological Disorders and Stroke; Contract grant number: NS050742 (to T.L.W.); Contract grant sponsor: Commission on Spinal Cord Research; Contract grant number: 08A-006-SCR3 (to K.R.M.).

We express our great appreciation to Dr. Steve Pfeiffer for his advice and input into the direction of our studies that led to the data relayed in this manuscript. His insights and enthusiasm encouraged us to pursue these questions. Most of all, we appreciate and will greatly miss Dr. Pfeiffer's inspiration in exploring so many new areas of oligodendrocyte and myelin biology. His enormous contributions to our work and to the advancement of knowledge in oligodendrocyte and myelin biology will always be remembered. We also thank Adam White and Antonio Valencia for invaluable discussions and advice on lipid raft isolation protocols, Robert Ledeen for help with GM-1 analysis, and Deborah Lazzarino for her helpful input into experiments and the manuscript.

References

Baron W, Decker L, Colognato H, ffrench-Constant C. Regulation of integrin growth factor interactions in oligodendrocytes by lipid raft microdomains. Curr Biol. 2003; 13:151–155. [PubMed: 12546790]

Carson MJ, Behringer RR, Brinster RL, McMorris FA. Insulin-like growth factor I increases brain growth and central nervous system myelination in transgenic mice. Neuron. 1993; 10:729–740. [PubMed: 8386530]

Chrysis D, Calikoglu AS, Ye P, D'Ercole AJ. Insulin-like growth factor-I overexpression attenuates cerebellar apoptosis by altering the expression of Bcl family proteins in a developmentally specific manner. J Neurosci. 2001; 21:1481–1489. [PubMed: 11222638]

Decker L, ffrench-Constant C. Lipid rafts and integrin activation regulate oligodendrocyte survival. J Neurosci. 2004; 24:3816–3825. [PubMed: 15084663]

Frederick TJ, Wood TL. IGF-I and FGF-2 coordinately enhance cyclin D1 and cyclin E-cdk2 association and activity to promote G_1 progression in oligodendrocyte progenitor cells. Mol Cell Neurosci. 2004; 25:480–492. [PubMed: 15033176]

Frederick TJ, Min J, Altieri SC, Mitchell NE, Wood TL. Synergistic induction of cyclin D1 in oligodendrocyte progenitor cells by IGF-I and FGF-2 requires differential stimulation of multiple signaling pathways. Glia. 2007; 55:1011–1022. [PubMed: 17508424]

Fu Q, Goodrum JF, Hayes C, Hostettler JD, Toews AD, Morell P. Control of cholesterol biosynthesis in Schwann cells. J Neurochem. 1998; 71:549–555. [PubMed: 9681444]

Gao X, Zhang J. Spatiotemporal analysis of differential akt regulation in plasma membrane microdomains. Mol Biol Cell. 2008 in press.

Gehrmann J, Yao DL, Bonetti B, Bondy CA, Brenner M, Zhou J, Kreutzberg GW, Webster HD. Expression of insulin-like growth factor-I and related peptides during motoneuron regeneration. Exp Neurol. 1994; 128:202–210. [PubMed: 8076663]

Gielen E, Baron W, Vandeven M, Steels P, Hoekstra D, Ameloot M. Rafts in oligodendrocytes: evidence and structure-function relationship. Glia. 2006; 54:499–512. [PubMed: 16927294]

Haugh JM, Meyer T. Active EGF receptors have limited access to PtdIns(4,5)P(2) in endosomes: implications for phospholipase C and PI3-kinase signaling. J Cell Sci. 2002; 115:303–310. [PubMed: 11839782]

Hur JY, Welander H, Behbahani H, Aoki M, Franberg J, Winblad B, Frykman S, Tjernberg LO. Active gamma-secretase is localized to detergent-resistant membranes in human brain. FEBS J. 2008; 275:1174–1187. [PubMed: 18266764]

Klein U, Gimpl G, Fahrenholz F. Alteration of the myometrial plasma membrane cholesterol content with beta-cyclodextrin modulates the binding affinity of the oxytocin receptor. Biochemistry. 1995; 34:13784–13793. [PubMed: 7577971]

Komoly S, Hudson LD, Webster HD, Bondy CA. Insulin-like growth factor I gene expression is induced in astrocytes during experimental demyelination. Proc Natl Acad Sci U S A. 1992; 89:1894–1898. [PubMed: 1371885]

Kramer EM, Schardt A, Nave KA. Membrane traffic in myelinating oligodendrocytes. Microsc Res Techniq. 2001; 52:656–671.

Lee AG. Myelin: delivery by raft. Curr Biol. 2001; 11:R60–R62. [PubMed: 11231143]

Lee SB, Hong SH, Kim H, Um HD. Co-induction of cell death and survival pathways by phosphoinositide 3-kinase. Life Sci. 2005; 78:91–98. [PubMed: 16154597]

Lee WH, Wang GM, Seaman LB, Vannucci SJ. Coordinate IGF-I and IGFBP5 gene expression in perinatal rat brain after hypoxia-ischemia. J Cereb Blood Flow Metab. 1996; 16:227–236. [PubMed: 8594054]

Levison, S., McCarthy, K. Astroglia in culture. In: Banker, G., Goslin, K., editors. Culturing nerve cells. Cambridge, MA: MIT Press; 1991. p. 309-336.

Lingwood D, Simons K. Detergent resistance as a tool in membrane research. Nat Protoc. 2007; 2:2159–2165. [PubMed: 17853872]

Lu X, Kambe F, Cao X, Yamauchi M, Seo H. Insulin-like growth factor-I activation of Akt survival cascade in neuronal cells requires the presence of its cognate receptor in caveolae. Exp Cell Res. 2008; 314:342–351. [PubMed: 18022157]

Macdonald JL, Pike LJ. A simplified method for the preparation of detergent-free lipid rafts. J Lipid Res. 2005; 46:1061–1067. [PubMed: 15722565]

Marta CB, Taylor CM, Coetzee T, Kim T, Winkler S, Bansal R, Pfeiffer SE. Antibody cross-linking of myelin oligodendrocyte glycoprotein leads to its rapid repartitioning into detergent-insoluble fractions, and altered protein phosphorylation and cell morphology. J Neurosci. 2003; 23:5461–5471. [PubMed: 12843245]

Marta CB, Taylor CM, Cheng S, Quarles RH, Bansal R, Pfeiffer SE. Myelin associated glycoprotein cross-linking triggers its partitioning into lipid rafts, specific signaling events and cytoskeletal rearrangements in oligodendrocytes. Neuron Glia Biol. 2004; 1:35–46. [PubMed: 16998591]

Marta CB, Bansal R, Pfeiffer SE. Microglial Fc receptors mediate physiological changes resulting from antibody cross-linking of myelin oligodendrocyte glycoprotein. J Neuroimmunol. 2008; 196:35–40. [PubMed: 18406472]

Mason JL, Xuan S, Dragatsis I, Efstratiadis A, Goldman JE. Insulin-like growth factor (IGF) signaling through type 1 IGF receptor plays an important role in remyelination. J Neurosci. 2003; 23:7710–7718. [PubMed: 12930811]

Matthews LC, Taggart MJ, Westwood M. Effect of cholesterol depletion on mitogenesis and survival: the role of caveolar and noncaveolar domains in insulin-like growth factor-mediated cellular function. Endocrinology. 2005; 146:5463–5473. [PubMed: 16166225]

Ness JK, Wood TL. Insulin-like growth factor I, but not neurotrophin-3, sustains Akt activation and provides long-term protection of immature oligodendrocytes from glutamate-mediated apoptosis. Mol Cell Neurosci. 2002; 20:476–488. [PubMed: 12139923]

Ness JK, Mitchell NE, Wood TL. IGF-I and NT-3 signaling pathways in developing oligodendrocytes: differential regulation and activation of receptors and the downstream effector Akt. Dev Neurosci. 2002; 24:437–445. [PubMed: 12666655]

Ness JK, Scaduto RC Jr, Wood TL. IGF-I prevents glutamate-mediated bax translocation and cytochrome C release in $O4^+$ oligodendrocyte progenitors. Glia. 2004; 46:183–194. [PubMed: 15042585]

Nishimura T, Inoue T, Shibata N, Sekine A, Takabe W, Noguchi N, Arai H. Inhibition of cholesterol biosynthesis by 25-hydroxycholesterol is independent of OSBP. Genes Cells. 2005; 10:793–801. [PubMed: 16098143]

Romanelli RJ, Wood TL. Directing traffic in neural cells: determinants of receptor tyrosine kinase localization and cellular responses. J Neurochem. 2008 in press.

Romanelli RJ, LeBeau AP, Fulmer CG, Lazzarino DA, Hochberg A, Wood TL. Insulin-like growth factor type-I receptor internalization and recycling mediate the sustained phosphorylation of Akt. J Biol Chem. 2007; 282:22513–22524. [PubMed: 17545147]

Saher G, Brugger B, Lappe-Siefke C, Mobius W, Tozawa R, Wehr MC, Wieland F, Ishibashi S, Nave KA. High cholesterol level is essential for myelin membrane growth. Nat Neurosci. 2005; 8:468–475. [PubMed: 15793579]

Schuck S, Honsho M, Ekroos K, Shevchenko A, Simons K. Resistance of cell membranes to different detergents. Proc Natl Acad Sci USA. 2003; 100:5795–5800. [PubMed: 12721375]

Simons K, Ikonen E. Functional rafts in cell membranes. Nature. 1997; 387:569–572. [PubMed: 9177342]

Song KS, Li S, Okamoto T, Quilliam LA, Sargiacomo M, Lisanti MP. Co-purification and direct interaction of Ras with caveolin, an integral membrane protein of caveolae microdomains. Detergent-free purification of caveolae microdomains. J Biol Chem. 1996; 271:9690–9697. [PubMed: 8621645]

Stam JC, Geerts WJ, Versteeg HH, Verkleij AJ, van Bergen en Hene-gouwen PM. The v-Crk oncogene enhances cell survival and induces activation of protein kinase B/Akt. J Biol Chem. 2001; 276:25176–25183. [PubMed: 11323409]

Taguchi K, Yoshinaka K, Yoshino K, Yonezawa K, Maekawa S. Biochemical and morphologic evidence of the interaction of oligodendrocyte membrane rafts with actin filaments. J Neurosci Res. 2005; 81:218–225. [PubMed: 15931670]

Vetrivel KS, Cheng H, Lin W, Sakurai T, Li T, Nukina N, Wong PC, Xu H, Thinakaran G. Association of gamma-secretase with lipid rafts in post-Golgi and endosome membranes. J Biol Chem. 2004; 279:44945–44954. [PubMed: 15322084]

Yao D, Liu X, Hudson L, Webster H. Insulin-like growth factor I treatment reduces demyelination and up-regulates gene expression of myelin-related proteins in experimental autoimmune encephalomyelitis. Proc Natl Acad Sci U S A. 1995; 92:6190–6194. [PubMed: 7541143]

Ye P, Carson J, D'Ercole AJ. In vivo actions of insulin-like growth factor-I (IGF-I) on brain myelination: studies of IGF-I and IGF binding protein-1 (IGFBP-1) transgenic mice. J Neurosci. 1995; 15:7344–7356. [PubMed: 7472488]

Ye P, Lee KH, D'Ercole AJ. Insulin-like growth factor-I (IGF-I) protects myelination from undernutritional insult: studies of transgenic mice overexpressing IGF-I in brain. J Neurosci Res. 2000; 62:700–708. [PubMed: 11104508]

Ye P, Li L, Richards RG, DiAugustine RP, D'Ercole AJ. Myelination is altered in insulin-like growth factor-I null mutant mice. J Neurosci. 2002; 22:6041–6051. [PubMed: 12122065]

Zeger M, Popken G, Zhang J, Xuan S, Lu QR, Schwab MH, Nave KA, Rowitch D, D'Ercole AJ, Ye P. Insulin-like growth factor type 1 receptor signaling in the cells of oligodendrocyte lineage is required for normal in vivo oligodendrocyte development and myelination. Glia. 2007; 55:400–411. [PubMed: 17186502]

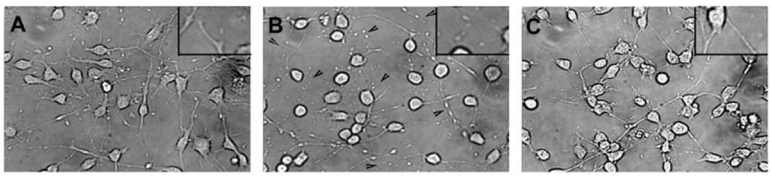

Fig. 1.

Cholesterol depletion alters OPC membrane integrity. OPCs were treated with 5 mM MβCD for 30 min at 37°C and were visualized by phase-contrast microscopy. **A:** Untreated cells exhibited normal, continuous processes extending from the cell body. **B:** Treatment with MβCD resulted in punctate, discontinuous processes (arrowheads). **C:** Posttreatment with 200 μM cholesterol–MβCD complexes reversed the effects of MβCD. **Insets** show magnified intact (A,C) or disrupted (B) processes.

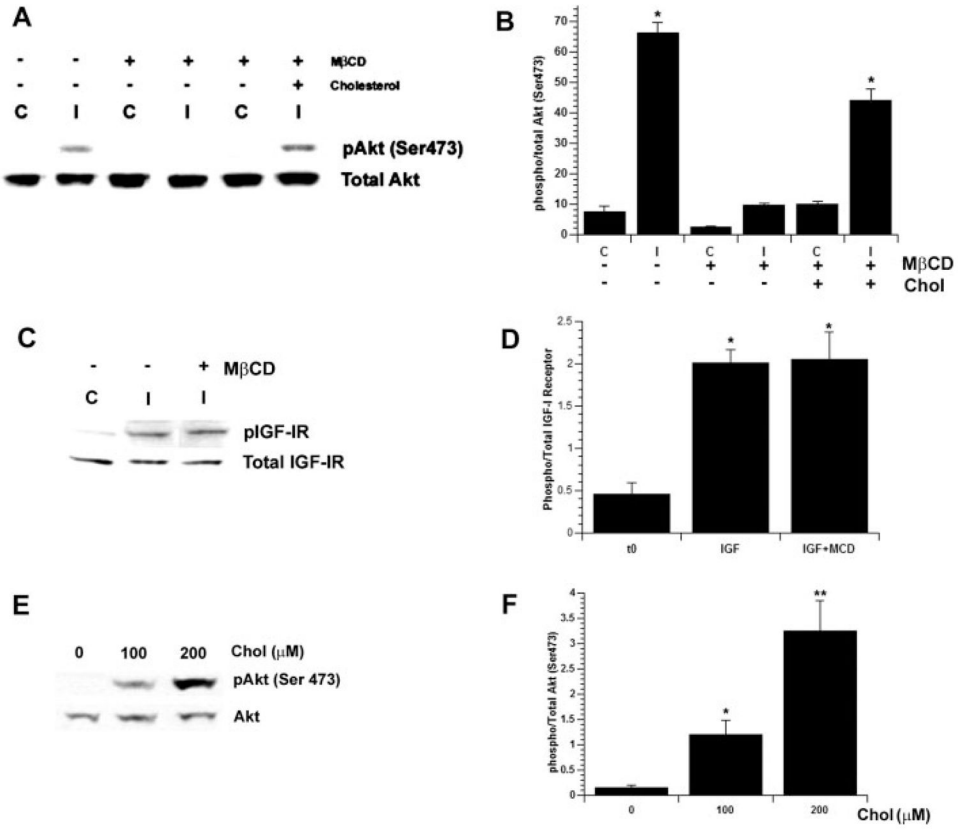

Fig. 2.

Acute cholesterol depletion blocks IGF-I-mediated Akt phosphorylation but not IGF-IR phosphorylation. OPCs were treated for 30 min with 10 ng/m IGF-I (C, control; I, IGF-I; with or without pretreatment with MβCD). Cell lysates were processed for SDS-PAGE and Western blot analysis. Data represent mean ± SEM (n = 3). **A–D:** Treatment with IGF-I induced phosphorylation of Akt (A,B; $P < 0.0001$). Pretreatment with MβCD blocked IGF-I-mediated Akt phosphorylation (A,B). Cholesterol repletion reversed the effects of MβCD (A,B; $P < 0.0001$). MβCD pretreatment had no effect on IGF-I-mediated IGF-IR phosphorylation compared with untreated control cells (C,D; $P < 0.003$). **E,F:** The recovery of Akt phosphorylation was dependent on the dose of cholesterol. Incubation with 200 μM cholesterol induced an approximately threefold increase in IGF-I-mediated Akt phosphorylation ($\star\star P < 0.008$) compared with incubation with 100 μM cholesterol (E,F; $\star P < 0.04$).

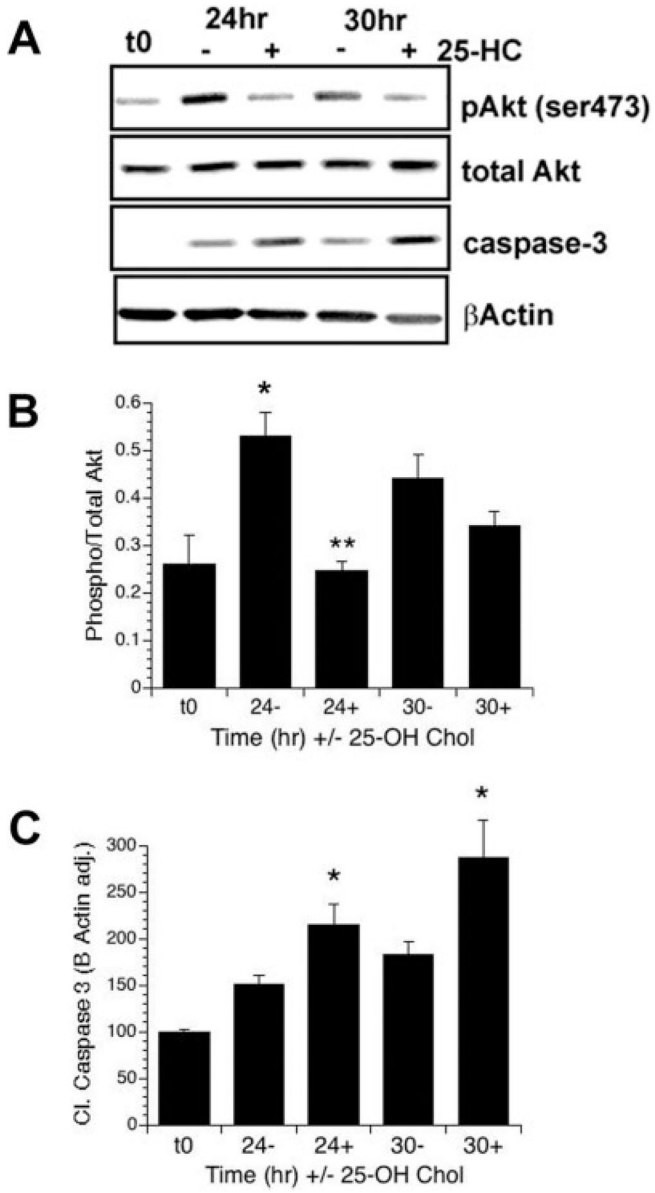

Fig. 3.

Inhibition of cholesterol biosynthesis blocks IGF-I-mediated sustained Akt phosphorylation. **A–C:** OPCs were treated with 10 ng/ml IGF-I in the presence (+) or absence (−) of 25-hydroxycholesterol (25-HC) for 24 or 30 hr in serum-free media. A: Representative Western blots showing levels of P-Akt, total Akt, cleaved caspase-3, and β-actin. B,C: Quantification of levels of Akt phosphorylation (B) and cleaved caspase-3 (E). Data represent the mean ± SEM from two experiments (n = 3 for t0; n = 5 for all other treatment groups). B: IGF-I stimulated the phosphorylation of Akt over control at 24 hr ($\star P = 0.02$, 24− vs. t0; $P = 0.06$ 30− vs. t0). Treatment with 25-HC completely prevented Akt phosphorylation at 24 hr ($\star\star P = 0.001$ 24+ vs. 24−). C: Treatment of OPCs with 25-HC resulted in a significant increase in cleaved caspase-3 at both 24 and 30 hr ($\star P = 0.03$ 24+ vs. 24−; $P = 0.04$ 30+ vs. 30−).

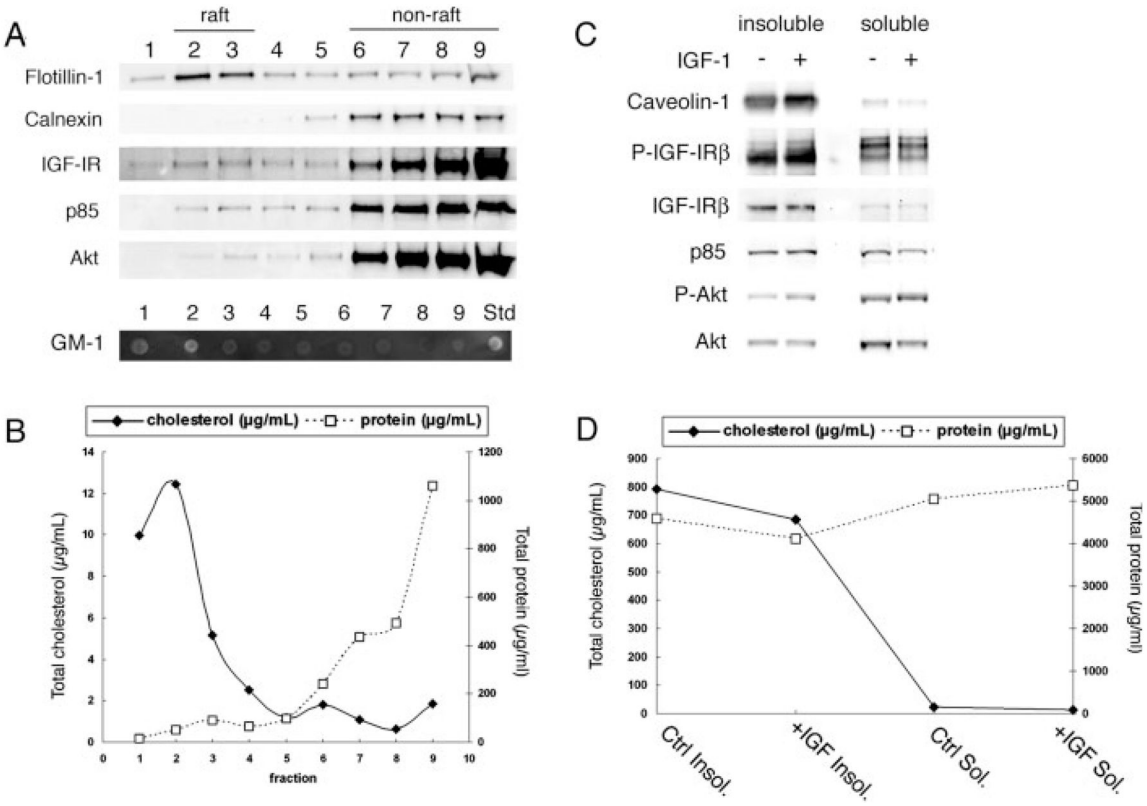

Fig. 4.

Isolation of detergent (Lubrol WX)-resistant membranes from OPCs. **A:** OPCs were lysed and solubilized in 0.5% Lubrol WX at 4°C. Lysates were mixed with 80% sucrose and subsequently overlaid with 35% and 5% sucrose. Sucrose gradients were centrifuged at 46,900 rpm for 18 hr at 4°C to separate buoyant raft membranes from bulk cellular material. Fractions 1–9 (equal volume) were taken from the top of each gradient and were used for SDS-PAGE and Western blot analysis. Flotillin-1, a marker for raft microdomains, was present in both buoyant "rafting" (2–3) fractions. GM-1 ganglioside, a raft marker, was detected in fractions 1 and 2 (GM-1 standard shown). Calnexin was localized only within nonbuoyant fractions. IGF-IR, p85, and Akt were detected strongly in nonbuoyant fractions but were also seen in buoyant fractions. **B:** Total cholesterol and protein distributions across fractions analyzed in A were determined as described in Materials and Methods. Squares (dashed line) represent total protein; lozenges (solid line) represent total cholesterol in each fraction. The majority of cholesterol is contained within the buoyant fractions. In contrast, the amount of protein per fractions is much greater in the nonbuoyant fractions. **C:** OPCs serum starved for 2 hr and treated or not with IGF-I (20 ng/ml) for 15 min were lysed and solubilized in 0.5% Lubrol WX at 4°C. Lysates were centrifuged at 13,000*g* for 20 min to separate detergent insoluble (caveolin-1- and cholesterol-enriched) fractions from the soluble supernatant. Equal protein fractions were analyzed by SDS-PAGE and Western blot analysis. Phosphorylated Akt and IGF-IR were increased in the insoluble fractions with IGF-I stimulation. Total Akt, IGF-1R, and p85 are also detected in insoluble fractions and were unchanged with IGF-I treatment. **D:** Total cholesterol (lozenges and solid line) and protein

(squares and dashed line) distribution in detergent insoluble and soluble fractions that correlate with fractions analyzed in C. Most cholesterol is contained within the Lubrol WX-insoluble fractions.